COMPARISON OF TWO GAS CHROMATOGRAPH MODELS AND ANALYSIS OF BINARY DATA

by

Paul S. Keba and Philip T. Woodrow

National Aeronautics and Space Administration

Grant NGL 33-018-091

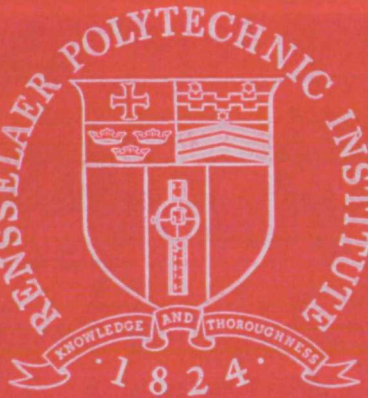

Rensselaer Polytechnic Institute

Troy, New York 12181

R.P.I. Technical Report MP-27

COMPARISON OF TWO GAS CHROMATOGRAPH MODELS AND ANALYSIS OF BINARY DATA

by

Paul S. Keba and Philip T. Woodrow

National Aeronautics and Space Administration

Grant NGL 33-018-091

July 15, 1972

School of Engineering
Rensselaer Polytechnic Institute
Troy, New York

ABSTRACT

One of the tasks to be undertaken by the unmanned missions to Mars is the search for chemical and biochemical species on the planet. Execution of this task requires a gas chromatograph-mass spectrometer system to separate and analyze sampled material. The overall objective of the gas chromatograph system studies is to generate fundamental design criteria and techniques to be used in the optimum design of the system. The particular tasks currently being undertaken are the comparison of two mathematical models of the chromatograph and the analysis of binary system data.

A previously developed chromatographic data reduction program is utilized to evaluate the predictions of two mathematical models, an equilibrium adsorption model and a non-equilibrium adsorption model. Using twenty sets of single component data, the two models are compared. On the basis of an average squared deviation between data and the prediction, the non-equilibrium model improves predictions marginally at best. Both models exhibit the same weaknesses in their inability to predict chromatogram spreading for certain systems. The heretofore neglected mechanism of intraparticle diffusion possibly accounts for the discrepencies and it will be studied in future modeling.

The analysis of binary data using the equilibrium adsorption model confirms that, for the systems considered, superposition of predicted single component behaviors is a first order representation of actual binary data. Composition effects produce non-idealities which limit the rigorous validity of superposition. This result poses additional questions as to prediction of multi-component chromatograms.

Both tasks -- model comparison and binary system analysis -- make use of newly implemented correlations for *a priori* system parameter estimation as required for data reduction.

CONTENTS

LIST OF TABLES

LIST OF FIGURES

I. INTRODUCTION

As pointed out by Sliva (1), an important task to be carried out by the unmanned missions to Mars is the search for organic matter and living organisms on the Martian surface. In order to fulfill this objective, it is presently planned to subject gaseous, liquid, and solid samples to biological and chemical reactions and subsequently to analyze the products. The analysis of these reaction products most likely will be carried out by a combination gas chromatograph-mass spectrometer. In order to define the fundamental system design criteria necessary for system optimization, a chromatographic system study -- both experimental and theoretical -- has been undertaken.

The chromatograph may be looked upon as a separating device where the phenomena of adsorption-desorption is utilized. Owing to the different characteristics of chemical species, each species will adsorb and desorb at different rates when exposed to a packed bed of granular particles with or without a liquid substrate. Because of the unique behavior of each chemical, a multi-component sample may be injected into a chromatograph and elute as separate waves of specific chemical species. Although the mechanisms involved in chromatograph operation have been well noted previous to this investigation, Figure 1 may serve as a graphic review. The sample is injected into a relatively inert carrier gas, helium in the case of the present studies. As this slug of sample passes through the chromatograph, the various species diffuse, adsorb, and desorb. Mass transfer of the chemicals to the adsorbing surface is represented by a dimensionless parameter N_{tOG} which is essentially determined by the system fluid mechanics. Adsorption and desorption is represented by a thermodynamic parameter mR_O which is peculiar to

CHROMATOGRAPHIC COLUMN CONCEPTS

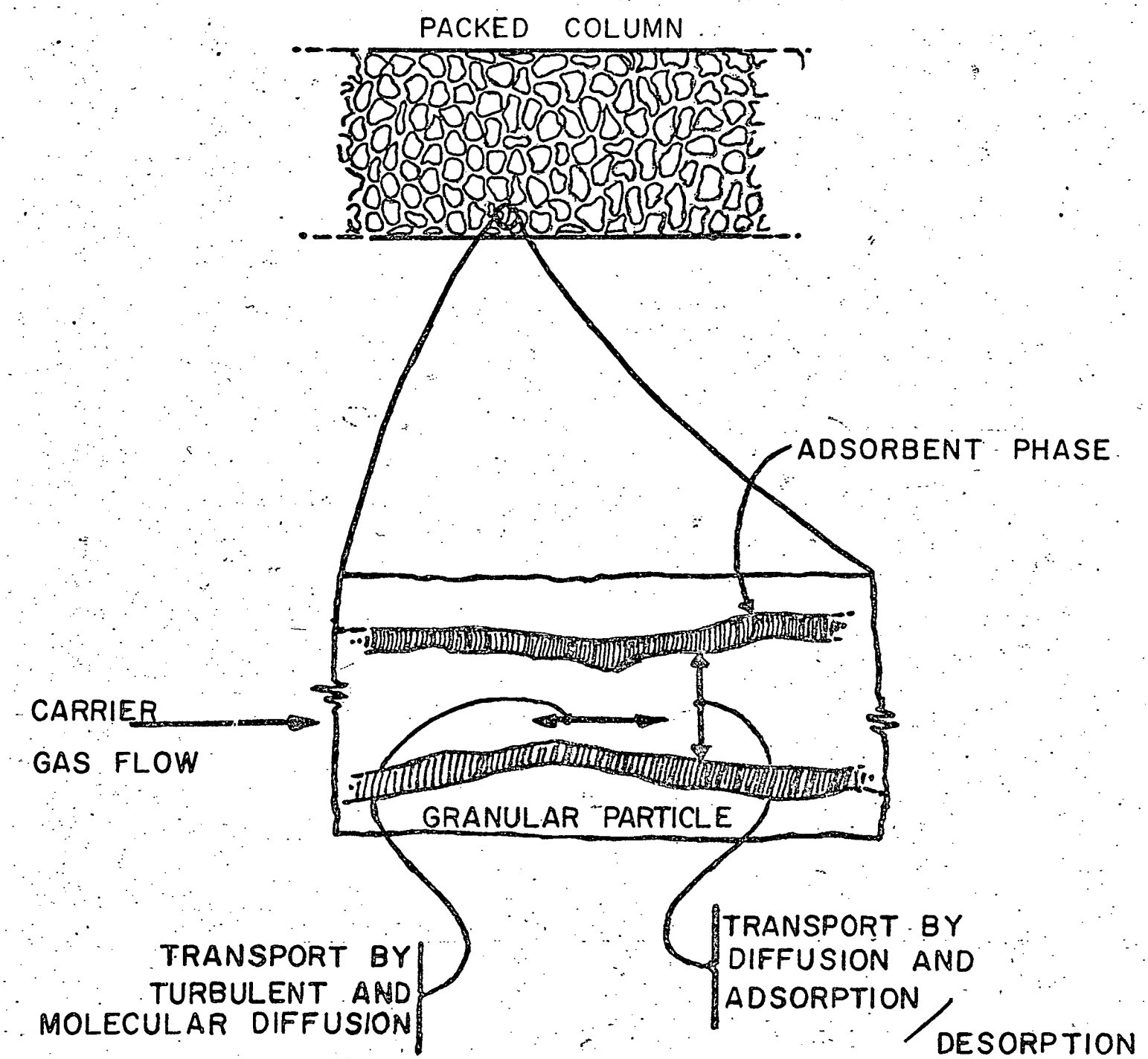

FIGURE 1

each species. Diffusion of the chemicals in the direction of the carrier gas flow is represented by the dimensionless parameter Pe which is also determined by the system fluid mechanics.

Prior work has produced several mathematical models of the chromatograph (1, 2, 3). These models were all derived from a fundamental, second-order partial differential equation set. Each model predicts the behavior of a component sample at the chromatograph column outlet based on an impulse injection.

Experimentally, data is obtained based on an input function which is a finite pulse. Thus, proper cognizance must be taken of the input form when comparing the prediction of a mathematical model to experimentally observed behavior. A basic tool for model verification and comparison was the result of Benoit's work (4). This tool is in the form of a computer program designated as the General Data Reduction Program (GDRP). Most importantly, this program will, given system input data, output data, parameters, and a mathematical model for the impulse response of the column, reduce the data to a consistent form and adjust the impulse response to a response which accounts for the finite nature of the input function. This adjustment is performed by numerical convolution of the impulse response with the actual input function. This allows a thoroughly consistent comparison of theoretical predictions to actual data.

The models to be analyzed and compared to data and to each other are called the Equilibrium Adsorption Model and the Non-Equilibrium Adsorption Model. Briefly, the difference in the two models lies in the fact that in the former, pointwise adsorption equilibrium is assumed throughout the column, while in the latter, a non-equilibrium situation

is assumed to exist. Further elucidation concerning both models is left to Section II.

As the actual chromatograph will most likely perform in a multi-component environment, experimental work has involved the analysis of binary systems. Further use of the GDRP has permitted study into whether principles of superposition are valid for prediction of chromatograph performance in the multi-component environment. In addition to this study, the analysis of binary data leads directly to areas of performance such as detectability and separability of multi-component samples.

II. SYSTEM MODELING

A. Theory and Background

Prior work in the area of mathematical models for the chromatographic system has been conducted by several investigators, (1,2,3). Several mathematical models based on different assumptions and of varying complexity have resulted. To date, these models have been based on a set of equations and boundary conditions which describe the behavior of a single, sample component in the chromatograph column:

Gas phase mass balance,

$$\frac{1}{Pe}\frac{\partial^2 y}{\partial z^2} - \frac{\partial y}{\partial z} - N_{tOG}(y - y^*) = \frac{\partial y}{\partial \theta} \qquad (1)^*$$

Adsorbed phase mass balance,

$$\frac{1}{R_O}\frac{\partial x}{\partial \theta} = N_{tOG}(y - y^*) \qquad (2)$$

*See Section VIII, Nomenclature, for definition of terms.

Thermodynamic relationship between the adsorbed and gas phases

$$y^* = mx \tag{3}$$

The above equations are valid under the following assumptions:

1. The column is isothermal.
2. The carrier gas velocity profile is flat.
3. The axial diffusion coefficient is a composite factor which may or may not have turbulent component.
4. The gas composition is approximately constant in the direction normal to flow; the concentration gradient occurs only in a thin boundary layer near the adsorbent; i.e., mass transfer coefficients can be used.
5. The adsorbent layer is so thin that there is no diffusional resistance within the layer in the direction normal to the surface.
6. The diffusivity in the adsorbent layer is so small that there is no diffusion in the direction parallel to the surface in the axial direction.
7. The net rate of adsorption for the carrier gas is negligible.
8. Only one component is adsorbed and its gas phase composition is very small.
9. The carrier gas behaves as an ideal gas.

The applicable boundary and initial conditions are as follows:

Initial conditions:

$$y(x,0) = 0$$

$$x(z,0) = 0$$

Boundary conditions:

$$y(0,\theta) = A_\delta$$

$$\lim_{z \to \infty} y(z,\theta) = \text{finite}$$

These conditions reflect a sample-free column at zero time, a sample injected as an impluse, and no end effects at the column exit.

The models to be considered are both second order models, i.e., the second order term in Equation 1 or axial diffusion is not neglected. The two models have been designated as the Equilibrium Adsorption Model and the Non-Equilibrium Adsorption Model, respectively. The difference in these two models lies in the fact the term N_{tOG} is taken to be infinite in the derivation of the Equilibrium Adsorption Model, and to be finite in the derivation of the Non-Equilibrium Adsorption Model. As described later, the different assumptions about N_{tOG} result in two models of completely different complexity, both mathematically and computationally.

B. Review of the Equilibrium Adsorption Model

Due to its simplicity, the Equilibrium Adsorption Model was used by Benoit (4) as the chromatograph model in the work to develop the initial form of the GDRP. The model itself has been considered in detail in another investigation (2). However, for the sake of completeness it is briefly reviewed.

The assumption of an infinite number of transfer units, i.e., $N_{tOG} = \infty$, also implies $y = y^*$ in Equation 1 and 2. This corresponds physically to pointwise equilibrium between the gas phase and the adsorbed phase of the packing. Mathematically, this assumption simplifies the

system equations so that a simple analytic solution is readily derived. The resultant model predicting component behavior at the column outlet is

$$y(1,\theta) = (A_\delta/2)\sqrt{\beta\, Pe/\pi\, \theta^3}\ \exp\left[-Pe(\theta-\beta)^2/4\beta\theta\right] \qquad (4)$$

Chromatogram predictions using this model are readily and efficiently evaluated in a straight forward manner. The computer routine, RESP, for this model has been documented elsewhere (5).

Although Benoit used this model in his investigation, the model is being used in this work for two reasons: re-evaluation of past data based on revisions in parameter estimating procedures and for comparison with the Non-Equilibrium Adsorption Model.

C. The Non-Equilibrium Adsorption Model

The Equilibrium Adsorption Model, which results from solutions of Equations 1, 2 and 3, assumes equilibrium gas phase compositions throughout the chromatograph column. As noted previously, this assumption corresponds to an infinite number of transfer units, N_{tOG}, which significantly simplifies the system equations and resultant solution -- a solution which offers few computational difficulties.

As the name implies, the Non-Equilibrium Adsorption Model assumes a non-equilibrium situation in the chromatograph column . This behavior is characterized by a finite number of transfer units, which complicates the final solution for component behavior.

Previous work has prompted further study of the Non-Equilibrium Adsorption Model for the chromatograph system. The use of the Equilibrium Adsorption Model by Benoit (4) in the GDRP resulted in good prediction of the basic characteristics of the data. However, an as yet undefined transport mechanism, temperature dependent in nature, resulted in

dispersion of the experimental output data as compared to the convolved impulse response of the Equilibrium Adsorption Model for certain systems, and model improvement was indicated.

Prior to this investigation, Taylor (3) studied and carried out initial development of the Non-Equilibrium Adsorption Model. However, the resulting computation scheme used for output chromatogram prediction was unstable for certain values of the system parameters. For this reason, and the need for a more extensive study of the Non-Equilibrium Adsorption Model, the model was re-evaluated using different numerical techniques and computational procedures. These different techniques and procedures have proved to be reliable and efficient, as well as directly applicable for use in the GDRP.

The general solution to Equations 1, 2, and 3, has been accomplished by adapting the work of Lapidus and Amundson (6) to the de-dimensionalized system of equations under consideration. The complete solution development appears in a recent report (5). The sample composition at the column outlet, as a function of dimensionless time, Θ, is as follows:

$$y(1,\Theta) = (A_\delta/2)\sqrt{Pe/\pi} \cdot \exp\left[Pe/2\right] \cdot \exp\left[-N_{tOG}\, mR_0\, \Theta\right]$$

$$\frac{d}{d\Theta}\int_0^\Theta \frac{I_0\left[2\sqrt{N_{tOG}^{\,2}\, mR_0(\Theta-x)x}\right]}{\sqrt{x^3}} \cdot \exp\left[-\left|(Pe/4x) + N_{tOG}\,(1-mR_0)x + (Pe\,x/4)\right|\right] \cdot dx \qquad (5)$$

Performing the indicated differentiation yields the final analytic form for the Non-Equilibrium Adsorption Model:

$$y(1,\theta) = c\,(y_1 + y_2) \tag{6}$$

where

$$c = (A_\delta/2)\sqrt{Pe/\pi} \cdot \exp(Pe/2) \cdot \exp(-N_{tOG}\, mR_0\, \theta) \tag{7}$$

$$y_1 = 1/\sqrt{\theta^3} \exp(-Pe/4\theta - Pe\theta/4 - N_{tOG}\theta + N_{tOG}\, mR_0\theta) \tag{8}$$

$$y_2 = 2N_{tOG}^{\,2}\, mR_0 \int_0^\theta \frac{I_1\left[2\sqrt{N_{tOG}^{\,2}\, mR_0(\theta-x)x}\right]}{\left[2\sqrt{N_{tOG}^{\,2}\, mR_0(\theta-x)x}\right]} \cdot \frac{1}{\sqrt{x}} \exp\left[-\left(Pe/4x + N_{tOG}(1-mR_0)x + Pe\cdot x/4\right)\right] \cdot dx \tag{9}$$

The behavior of the integral in Equation (9) at the endpoints appears to offer a problem in computation. However, the integrand has limiting values at the endpoints, as noted by Taylor (3), although the actual computational scheme to be used in this investigation never requires direct evaluation at the integral endpoints. Although the integral in Equation (9) is comprised of well known functions, its numerical evaluation is not trivial. The following analysis shows why an involved treatment is necessary and indicates how this is implemented to yield the appropriate results.

The expression for $y(1,\theta)$, Equation (6) can be rewritten to yield:

$$y(1,\theta) = cy_1 + cy_2 \tag{10}$$

From Equations 7 and 8 one obtains:

$$cy_1 = (A_\delta/2)\sqrt{Pe/\pi\theta^3} \exp(Pe/2 - Pe/4\theta - Pe\theta/4 - N_{tOG}\theta) \tag{11}$$

Evaluation of this expression is straight forward as long as the exponential argument is checked for large negative values during computation. Except in cases of low N_{tOG} and low Peclet numbers, Pe, the contribution of cy_1 to the total impulse response is generally negligible.

Evaluation of cy_2 is more involved. From the previous expressions, cy_2 can be written in the following form:

$$cy_2 = (A_\delta/2)\sqrt{Pe/\pi} \cdot 2N_{tOG}^{\ 2}\, mR_0 \cdot \exp(-N_{tOG}\, mR_0\theta) \cdot \int_0^\theta \frac{I_1(Arg)}{(Arg)} \frac{1}{\sqrt{x}} \cdot \exp\left[Pe/2 - (Pe/4x + N_{tOG}(1-mR_0)x + Pex/4)\right] \cdot dx \qquad (12)$$

where:

$$Arg = 2\sqrt{N_{tOG}^{\ 2}\, mR_0(\theta - x)\, x} \qquad (13)$$

Two approximations for the modified Bessel function of the first kind and order one are used (7). These involve large and small argument expressions. If t is defined as $(Arg/3.75)$, then

$$I_1(Arg) = Arg(A_1 + A_2t^2 + A_3t^4 + A_4t^6 + A_5t^8 + A_6t^{10} + A_7t^{12} + \epsilon) \qquad (14)$$

$$\text{for } -3.75 \leq Arg \leq 3.75$$

$$\text{and } |\epsilon| < 8 \times 10^{-9}$$

and

$$I_1(Arg) = \exp(Arg)/\sqrt{Arg} \cdot \left[B_1 + B_2t^{-1} + B_3t^{-2} + B_4t^{-3} + B_5t^{-4} + B_6t^{-5} + B_7t^{-6} + B_8t^{-7} + B_9t^{-8} + \epsilon\right] \qquad (15)$$

$$\text{for } 3.75 \leq \text{Arg} < \infty$$

$$\text{and } |e| < 2.2 \times 10^{-7}$$

The coefficients in the above two expressions, are given in Table I.

The behavior of Arg, as defined in Equation 13 was studied. It was noted that within the range of computed responses, integration variable, x, and parameters encountered, it was reasonable to use the large argument polynomial expression, Equation 15, for the Bessel function. For example, for $mR_0 = 0.2$, $\theta = 5$, $x = 1$, (This is an integration variable value near the maximum of the integrand), and setting $\text{Arg} = 3.75$ requires the value of N_{tOG} to be on the order of 2.1. This value is several orders of magnitude less than any N_{tOG} value encountered to date, and it is not anticipated that such low N_{tOG} values will occur in practical designs.

Therefore it is appropriate to consider Equation 15 for $I_1(\text{Arg})$ in the following development. Denoting the polynomial in Equation 15 by POLYB, the expression becomes:

$$I_1(\text{Arg}) = \exp(\text{Arg})\ \text{POLYB}/\sqrt{\text{Arg}} \tag{16}$$

Equation 12, after rearrangement, yields:

$$cy_2 = \int_0^{\theta} \frac{\text{POLYB}}{\sqrt{\text{Arg}^3}} \cdot \frac{1}{\sqrt{x}} \cdot \exp\left[F(x)\right] \cdot dx \tag{17}$$

where

$$F(x) = \left[-N_{tOG}^2\left(\sqrt{x} - \sqrt{mR_0(\theta-x)}\right)^2 - (Pe/4x)(x-1)^2 + \ln(A_\delta N_{tOG}^2\, mR_0 \sqrt{Pe/\pi})\right] \tag{18}$$

TABLE I

COEFFICIENTS FOR POLYNOMIAL APPROXIMATION
OF MODIFIED BESSEL FUNCTION

A_1	= 0.50	B_1	= 0.39894228
A_2	= 0.87890594	B_2	= -0.03988024
A_3	= 0.51498869	B_3	= -0.00362018
A_4	= 0.15084934	B_4	= 0.00163801
A_5	= 0.02658733	B_5	= -0.01031555
A_6	= 0.00301532	B_6	= 0.02282967
A_7	= 0.00032411	B_7	= -0.02895312
		B_8	= 0.01787654
		B_9	= -0.00420059

It is reasonable to expect the exponential in the integrand of Equation 17 to completely dominate the behavior of the entire integrand. This is, in fact, the case. Hence, the behavior of the exponential argument, $F(x)$, is very important. If one examines the expression for $F(x)$, one notes that it will have a maximum in the neighborhood of $x = 1$. Also, although not directly obvious from Equation 18 the behavior of $F(x)$ is very peaked, and hence, the exponential is very peaked in the neighborhood of its maximum. Table II shows how dramatic this functional behavior is; i.e., for the noted values of the parameters mR_0, N_{tOG}, Pe, and θ, the exponential ranges from approximately zero to fifty million and back to zero for the integration variable range of 0.87 to 1.12.

This region of the integration variable as determined by the exponential argument study brings about an interesting conclusion. By recognizing that the integrand behavior is dominated by the exponential term, one may reduce the computational work involved in evaluation of cy_2 by reducing the range of integration. Alternative to integrating from 0 to θ, one may integrate from some x_1 to x_2 or symbolically

$$\int_0^{\theta} f(x)\,dx \longrightarrow \int_{x_1}^{x_2} f(x)\,dx$$

because outside the range $x_1 \leq x \leq x_2$, the integrand is effectively zero based on the previous study. For computational purposes, it is necessary to have a generalized method of selecting the integration region, $\left[x_1, x_2\right]$, for each value of θ in the total response calculation. In addition, it has been noted that for a particular value of

TABLE II

TYPICAL BEHAVIOR OF EXPONENTIAL ARGUMENT IN INTEGRAND OF NON-EQUILIBRIUM ADSORPTION MODEL

Integration Variable x	F(x)	exp[F(x)]
0.8675	-25.294	0.000000
0.8775	-19.153	0.000000
0.8875	-13.450	0.000001
0.8975	- 8.193	0.000277
0.9075	- 3.392	0.033639
0.9175	0.943	2.568731
0.9275	4.804	122.035800
0.9375	8.181	3573.371000
0.9475	11.065	63884.840000
0.9575	13.446	690757.500000
0.9675	15.314	4474208.000000
0.9775	16.660	17194670.000000
0.9875	17.475	38831070.000000
0.9975	17.748	51033130.000000
1.0075	17.470	38651950.000000
1.0175	16.631	16706390.000000
1.0275	15.222	4080403.000000
1.0375	13.231	557618.800000
1.0475	10.651	42215.150000
1.0575	7.469	1752.914000
1.0675	3.677	39.524000
1.0775	- 0.736	0.479071
1.0875	- 5.780	0.003090
1.0975	-11.464	0.000011
1.1075	-17.780	0.000000
1.1175	-24.797	0.000000

Note: $\theta = 5.5$

$mR_0 = 0.22$

$Pe = 7800.0$

$N_{tOG} = 2200.0$

N_{tOG} and Pe, the reduced integration is extremely sensitive to values of the parameter mR_0. Table III shows the almost logarithmic dependence of reduced integration range on mR_0. This in turn affects the desirable integration variable increment to be used in actual numerical integration of the integral yielding cy_2.

One can say that the maximum integrand value occurs at the maximum value of $F(x)$, the exponential argument. Thus, it is desirable to know an x_0 such that $F(x_0) = F_{maximum}$, for a given value of θ and parameters mR_0, Pe, and N_{tOG}. This occurs when the first derivative of $F(x)$ with respect to the x evaluated at x_0 is zero; i.e., $F'(x_0) = 0$. Thus, it is appropriate to have a technique to solve for the zero of the function $F'(x)$. This is accomplished numerically using Newton's method (8).

Once knowing the value of the integration variable that maximizes the integrand exponential, the range of integration is determined based on the values of $F(x)$, i.e., stepping forward and backward from x until $F(x)$ decreases to a large negative number.

Thus, the actual integration yielding cy_2 may be carried out based on the reduced integration range. Romberg integration with Richardson extrapolation is used for this computational step (8).

The implementation of the preceding computational techniques appears as a computer subprogram, RESP. This is the general name given to a routine which computes an impulse response for a particular mathematical model in the GDRP. Further details about the program appear in a recent report (5).

TABLE III

EFFECT OF mR_0 ON INTEGRATION RANGE FOR
θ-VALUE NEAR PEAK OF CHROMATOGRAM

mR_0	θ	Integration range selected*
0.2	6.00	0.08
0.8	2.25	0.05
2.0	1.50	0.031
10.0	1.10	0.010
50.0	1.025	0.002
80.0	1.00	0.0012
200.0	1.00	0.0005
500.0	1.00	0.0002
800.0	1.00	0.0002
1000.0	1.00	0.0002

Conditions: $N_{tOG} = 92,450$; Pe = 8333

*Basis: where exponential argument of integrand of cy_2 becomes less than -20.0.

III. PARAMETER ESTIMATION

The use of mathematical models for predicting the behavior of a chromatograph requires the a priori knowledge of the values of the system parameters which are inherent in each model. The Equilibrium Adsorption Model requires a priori knowledge of the Peclet number, Pe, and mR_0, while the Non-Equilibrium Adsorption Model requires a priori knowledge of Pe, mR_0, and N_{tOG}, the number of transfer units.

The Peclet number is a dimensionless parameter which is indicative of the axial diffusion of the component samples and is defined as:

$$Pe = \bar{v} L/D \tag{19}$$

The Peclet number is a function of the fluid mechanics of the system and the physical properties of the system. The Reynolds number, Re represents the fluid mechanics of the system, while the Schmidt number Sc, embodies the physical properties of the system in current estimating procedures.

For the chromatograph, the Reynolds number is based on the particle diameter and the superficial velocity or,

$$Re = d\, v \rho/\mu \tag{20}$$

A mean velocity is used in Equation 20 because pressure drop along the length of the column changes the local density and velocity and is estimated as follows (9):

$$\frac{v}{v_{avg}} = \left(\frac{3}{4}\right) \left[\frac{1+2(Po/Pi)+(Po/Pi)^2}{1+ (Po/Pi)+(Po/Pi)^2}\right] \tag{21}$$

where v_{avg} is the velocity based on arithmetic average of the column inlet and output pressures.

The Schmidt number is defined as

$$Sc = \mu/\rho D_m \tag{22}$$

Calculation of the molecular diffusion, D_m, is accomplished by using the Wilke-Lee modification (10) of the Hirschfelder, Bird, and Spotz method (11) with the Bird, Hirschfelder, and Curtiss correction (12) for polar-nonpolar interactions. A Hirschfelder, Bird and Spotz method (11) for temperature extrapolation of the viscosity is used.

Upon calculation of Reynolds and Schmidt numbers, the Peclet number may be estimated by a correlation proposed by Gunn (13):

$$L/dPe = Re\ Sc\ (1 - p)^2/\epsilon\Gamma + \left[Re^2Sc^2p(1-p)^2/\epsilon^2\Gamma^2\right]\left[\exp(-\epsilon\Gamma/p(1-p)ReSc)-1\right] + \epsilon/\tau\ Re\ Sc \tag{23}$$

where p is a probability parameter correlated by Gunn (13).

The number of transfer units, N_{tOG} is a dimensionless parameter which characterizes mass transfer between the component in the vapor phase and the component adsorbed on the chromatograph packing. As a measure of adsorption, an infinite value of N_{tOG} indicates equilibrium adsorption while a finite N_{tOG} indicates non-equilibrium adsorption. The basic expression for N_{tOG} in packed beds is:

$$N_{tOG} = Sh \cdot (aL)/Sc \cdot Re \tag{24}$$

Estimation of the Sherwood number, Sh, is accomplished using a correlation proposed by Wakao, Oshima, and Yagi (14). For Reynolds numbers less than 100, which is the usual flow regime in chromatographic columns,

The correlation becomes

$$Sh = 2.0 + 1.45\ Sc^{1/3} \cdot Re^{1/2} \qquad (25)$$

Thus, use of this equation in Equation 24 yields the final estimate for N_{tOG} used in this investigation.

The calculations required to obtain values of the Pe and N_{tOG} parameters have been implemented in a computer program. This program estimates various physical and transport properties of a binary, gaseous chromatograph system in which the bulk properties are those of the carrier gas. The program documentation has appeared elsewhere (5).

Another parameter which enters the solution of the chromatographic differential equations is mR_0, a thermodynamic parameter which represents the adsorption characteristics of the specific chemical system that is being considered. For a given component, it specifies the approximate position along the time axis where the maximum point occurs. The value of mR_0 for each component is determined by matching the occurrence of the maximum composition of the convolved output for the particular chromatograph model being considered with the time that the maximum composition is observed in the experimental data of that particular system. The matching is accomplished by the use of an iterative regula falsi method (8, 15) in the GDRP and details have been reported earlier (4).

IV. ANALYSIS OF SUPERPOSITION

The chromatograph will in general be used with multicomponent systems. In addition to evaluating the mathematical models with chromatograms from single component systems, it is an objective of this task to apply the models to mixtures of several chemicals.

A logical extension of the system model, Equations 1, 2, and 3, is to utilize the principle of superposition. Superposition assumes that each component is independent and that single component data may be used in multicomponent systems by solving for each component separately. Furthermore, it is assumed that coupling between the set of equations 1, 2, and 3 written in vector form is negligible. This is a particularly important assumption when considering the adsorption isotherm, Equation 3.

In this study, superposition is implemented by first computing the output responses for the pure components using the Equilibrium Adsorption Model, Equation 4, and assuming the concentrations in the measured input injection signal are completely uniform with respect to time. The predicted output compositions of each component are adjusted in proportion to the amount of the component present in the sample. The actual output data for each component are normalized and adjusted similarly. Visual and numerical comparison of the predicted and experimental chromatograms can then be made.

The superposition calculations and curve plotting are performed by the computer and programming details have been presented elsewhere (5).

V. RESULTS AND DISCUSSION

A. Column Characteristics

Table IV lists the characteristics of the various columns used in obtaining the experimental chromatographic data with which the model comparisons were made. Included in this table are the length of the column, the inside and outside diameters of the column, and the diameter of the particles within the column. The range of the temperature over which the column is to be used is noted. The composition of the material within the column is given along with an outline of the substances that the column will separate.

TABLE IV

CHROMATOGRAPHIC COLUMN CHARACTERISTICS

Designation	Chromosorb 102	Molecular Sieve 5A	Carbowax 1500/ Chromosorb P
Composition	Microporous styrene divinyl - benzene polymers	Synthetic zeolite	Polyethylene glycol (20% by weight) on diatomaceous earth
Temperature range	to 250°C	to 350°C	to 225°C
Application	Separation of low molecular weight highly polar substances	Separation of light gases	Separation of high boiling, polar compounds

Length - 100 cm; outside diameter - 0.32 cm; inside diameter - 0.22 cm; particle size - 0.025/0.018 cm

B. Experimental Conditions - Single Component Data

Comparisons were made for single component systems between actual chromatograms and the convolved output response obtained using, first, the Equilibrium Adsorption Model, and second, the Non-Equilibrium Adsorption Model. The source of the data used in these calculations was the work of Benoit (4). Table V gives the experimental conditons of the single component studies. For each run the component, the carrier gas flow rate, the temperature and the column used are listed.

C. System Parameter Estimations

In order to simplify the calculations involved in obtaining the various physical properties and transport parameters, the previously mentioned computer program was utilized. Table VI lists the physical properties of the carrier gas and the sample for the single component experiments. The molecular weight, the molecular radius, the E/K factor, the dipole moment, and the dielectric constant of the carrier and trace gases are given along with the viscosity of the carrier gas as measured at a standard temperature. Tables VI also lists for each run experimental conditions such as temperature, pressure, and helium flow rates and column characteristics such as particle diameter, tube diameter, and length. Included in the print out are the velocity, Reynolds number, Schmidt number, Peclet number, and the number of transfer units.

D. Equilibrium Adsorption Model and Non-Equilibrium Adsorption Model GDRP Results

Figures 2 through 5 show typical comparisons between convolved output for the Equilibrium Adsorption Model and the experimental chromatograms. The Non-Equilibrium Adsorption Model gives similar

TABLE V

EXPERIMENTAL CONDITIONS: SINGLE COMPONENT STUDIES

Component	Column	Helium Flow Rates cu cm/min	Temperature deg C
Nitrogen	Molecular Sieve	35	20
Oxygen	Molecular Sieve	35	20
Pentane	Chromosorb 102	32.2	150
Pentane	Chromosorb 102	20	200
Heptane	Chromosorb 102	32.2	150
Heptane	Chromosorb 102	20	200
Acetone	Chromosorb 102	24	125
Acetone	Chromosorb 102	43	100-200
Ethylene	Chromosorb 102	38	20
Ethylene	Chromosorb 102	43	28-175

TABLE VI

SYSTEMS PARAMETERS

COMPONENT	M.W.	R A	E/K DEG K	DIPOLE MOMENT	DIELECTRIC CONSTANT	(VIS)STD MICROPOISE	(T)STD DEG K
HELIUM	4.00	2.551	10.22	0.0	1.0000511	194.1	293.2
NITROGEN	28.01	3.798	71.40	0.0	1.0004305		

TEMP DEG K	PRES PSIA	FLOW CC/MIN	(VEL)BED CM/SEC	PARTICLE DIA, CM	TUBE DIA, CM	LENGTH CM	REYNOLDS NUMBER	SCHMIDT NUMBER	PECLET NUMBER	NTOG
301.2	35.40	35.0	21.794	0.0214	0.22	100.0	0.2608E 00	1.7149	0.7069E 04	0.1086E 06

COMPONENT	M.W.	R A	E/K DEG K	DIPOLE MOMENT	DIELECTRIC CONSTANT	(VIS)STD MICROPOISE	(T)STD DEG K
HELIUM	4.00	2.551	10.22	0.0	1.0000511	194.1	293.2
OXYGEN	32.00	3.467	106.70	0.0	1.0003886		

TEMP DEG K	PRES PSIA	FLOW CC/MIN	(VEL)BED CM/SEC	PARTICLE DIA, CM	TUBE DIA, CM	LENGTH CM	REYNOLDS NUMBER	SCHMIDT NUMBER	PECLET NUMBER	NTOG
301.2	35.40	35.0	21.794	0.0214	0.22	100.0	0.2608E 00	1.5989	0.6620E 04	0.1156E 06

COMPONENT	M.W.	R A	E/K DEG K	DIPOLE MOMENT	DIELECTRIC CONSTANT	(VIS)STD MICROPOISE	(T)STD DEG K
HELIUM	4.00	2.551	10.22	0.0	1.0000511	194.1	293.2
N-PENTANE	72.15	5.784	341.10	0.100	1.0020000		

TEMP DEG K	PRES PSIA	FLOW CC/MIN	(VEL)BED CM/SEC	PARTICLE DIA, CM	TUBE DIA, CM	LENGTH CM	REYNOLDS NUMBER	SCHMIDT NUMBER	PECLET NUMBER	NTOG
423.2	27.30	32.2	34.485	0.0214	0.22	100.0	0.1977E 00	3.4539	0.1034E 05	0.7328E 05
473.1	23.20	20.0	26.886	0.0214	0.22	100.0	0.1157E 00	3.4421	0.6341E 04	0.1159E 06

TABLE VI

(concluded)

COMPONENT	M.W.	R A	E/K DEG K	DIPOLE MOMENT	DIELECTRIC CONSTANT	(VIS)STD MICROPOISE	(T)STD DEG K
HELIUM	4.00	2.551	10.22	0.0	1.0000511	194.1	293.2
N-HEPTANE	100.21	6.480	405.10	0.100	1.0027000		

TEMP DEG K	PRES PSIA	FLOW CC/MIN	(VEL)BED CM/SEC	PARTICLE DIA, CM	TUBE DIA, CM	LENGTH CM	REYNOLDS NUMBER	SCHMIDT NUMBER	PECLET NUMBER	NTOG
423.2	27.30	32.2	34.485	0.0214	0.22	100.0	0.1977E 00	4.1452	0.1201E 05	0.6231E 05
473.1	23.20	20.0	26.886	0.0214	0.22	100.0	0.1157E 00	4.1293	0.7519E 04	0.9826E 05

COMPONENT	M.W.	R A	E/K DEG K	DIPOLE MOMENT	DIELECTRIC CONSTANT	(VIS)STD MICROPOISE	(T)STD DEG K
HELIUM	4.00	2.551	10.22	0.0	1.0000511	194.1	293.2
ACETONE	58.08	3.829	428.00	2.880	1.0116000		

TEMP DEG K	PRES PSIA	FLOW CC/MIN	(VEL)BED CM/SEC	PARTICLE DIA, CM	TUBE DIA, CM	LENGTH CM	REYNOLDS NUMBER	SCHMIDT NUMBER	PECLET NUMBER	NTOG
398.2	35.30	24.0	19.804	0.0214	0.22	100.0	0.1494E 00	2.0539	0.4938E 04	0.1487E 06
373.2	44.70	43.0	27.258	0.0214	0.22	100.0	0.2718E 00	2.0604	0.8689E 04	0.8896E 05
398.2	47.10	43.0	27.739	0.0214	0.22	100.0	0.2595E 00	2.0539	0.8309E 04	0.9276E 05
423.2	49.25	43.0	28.335	0.0214	0.22	100.0	0.2483E 00	2.0490	0.7965E 04	0.9647E 05
448.2	51.60	43.0	28.761	0.0214	0.22	100.0	0.2383E 00	2.0444	0.7652E 04	0.1001E 06
473.2	53.50	43.0	29.319	0.0214	0.22	100.0	0.2298E 00	2.0406	0.7388E 04	0.1034E 06

COMPONENT	M.W.	R A	E/K DEG K	DIPOLE MOMENT	DIELECTRIC CONSTANT	(VIS)STD MICROPOISE	(T)STD DEG K
HELIUM	4.00	2.551	10.22	0.0	1.0000511	194.1	293.2
ETHYLENE	28.05	4.163	224.70	0.0	1.0014800		

TEMP DEG K	PRES PSIA	FLOW CC/MIN	(VEL)BED CM/SEC	PARTICLE DIA, CM	TUBE DIA, CM	LENGTH CM	REYNOLDS NUMBER	SCHMIDT NUMBER	PECLET NUMBER	NTOG
299.1	35.30	38.0	23.559	0.0214	0.22	100.0	0.2844E 00	2.1123	0.9250E 04	0.8378E 05
301.2	37.30	43.0	25.651	0.0214	0.22	100.0	0.3185E 00	2.1118	0.1021E 05	0.7627E 05
323.2	39.10	43.0	26.464	0.0214	0.22	100.0	0.3028E 00	2.1056	0.9744E 04	0.7975E 05
348.2	40.30	43.0	27.794	0.0214	0.22	100.0	0.2877E 00	2.0998	0.9294E 04	0.8343E 05
373.2	44.70	43.0	27.258	0.0214	0.22	100.0	0.2718E 00	2.0952	0.8821E 04	0.8765E 05
398.2	47.10	43.0	27.739	0.0214	0.22	100.0	0.2595E 00	2.0913	0.8446E 04	0.9127E 05
423.2	49.25	43.0	28.335	0.0214	0.22	100.0	0.2483E 00	2.0878	0.8102E 04	0.9487E 05
448.2	51.60	43.0	28.761	0.0214	0.22	100.0	0.2383E 00	2.0852	0.7793E 04	0.9834E 05

results. Similar figures and selected tabular data for all experiments appear elsewhere (5).

Figure 2 shows that the acetone-Chromosorb 102 system is well represented by the model at 175°C. Similar results were obtained over the temperature range of 100 to 200°C, with the simulation more closely representing the experimental data at the higher temperatures.

As seen in Figure 3, the ethylene-chromosorb 102 system is not as well simulated by the proposed models. Since the area under each chromatograms is proportional to the size of the injected sample and hence the two areas are identical, it appears other mechanisms in the chromatographic process are occurring. Similar results were obtained over the temperature range 28 to 175°C with the simulation being slightly better at the lower temperatures.

Pentane and heptane on Chromosorb 102 were studied as a binary, multicomponent system and the chromatograms of the pure compounds at 200°C appear in Figures 4 and 5. Pentane is well represented by the model whereas representation of the heptane is less adequate.

E. Quantitative Comparison of the Two Models

Qualitatively, representation of the experimental chromatograms by the Equilibrium and Non-Equilibrium Adsorption Models are equivalent. For quantitative comparison, the average squared deviation between the particular model's convolved response and the actual output data is used. This squared deviation is obtained over that portion of time where finite responses occur, not over the entire time domain.

Results of the computation of the average squared deviation between the convolved model response and the data are presented in Table VII for both models and all of the twenty pure component systems used. The information in Table VII confirms the qualitative observations

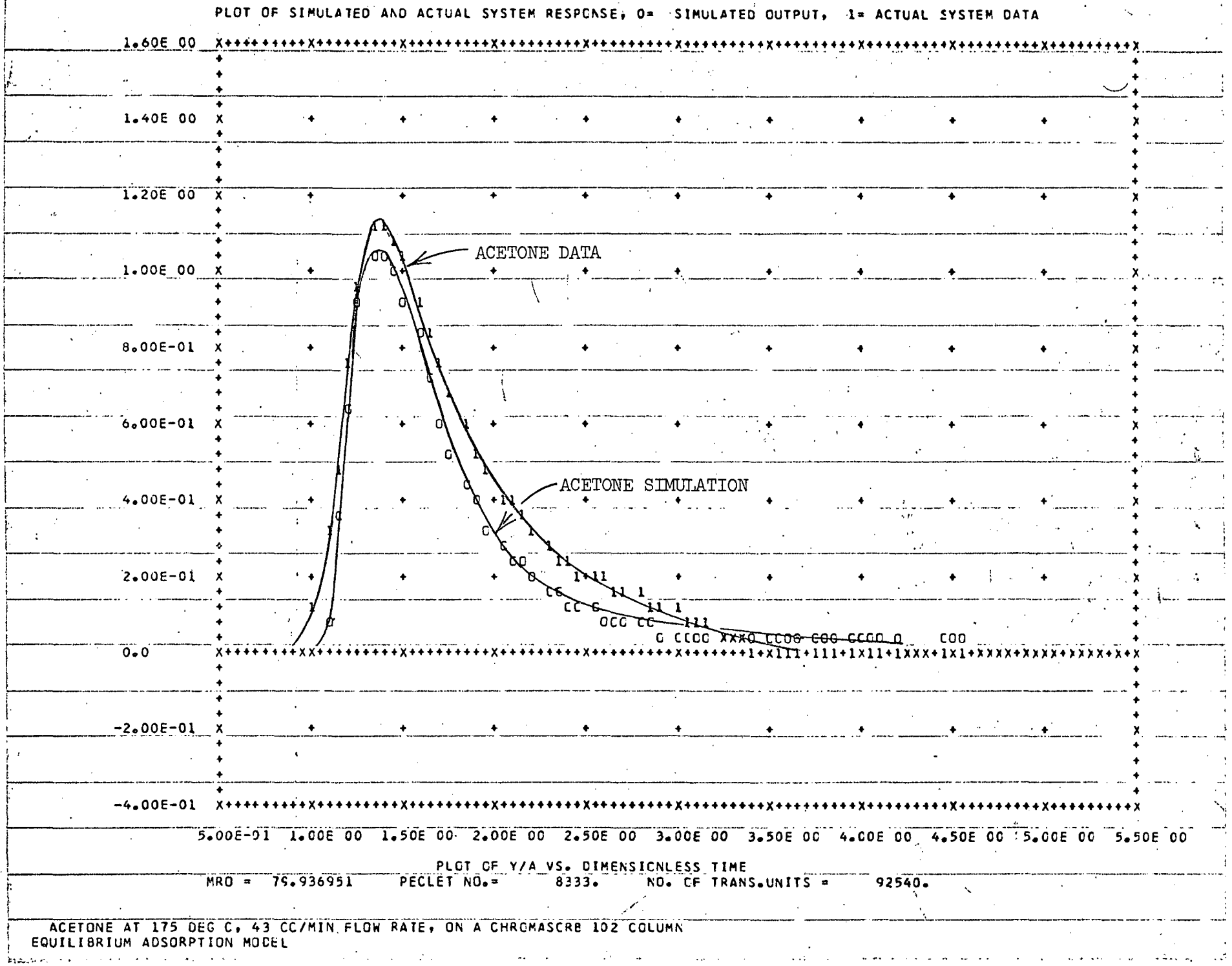

Figure 2 Comparison of Predicted and Actual Chromatograms for Acetone on Chromosorb 102 at 175°C

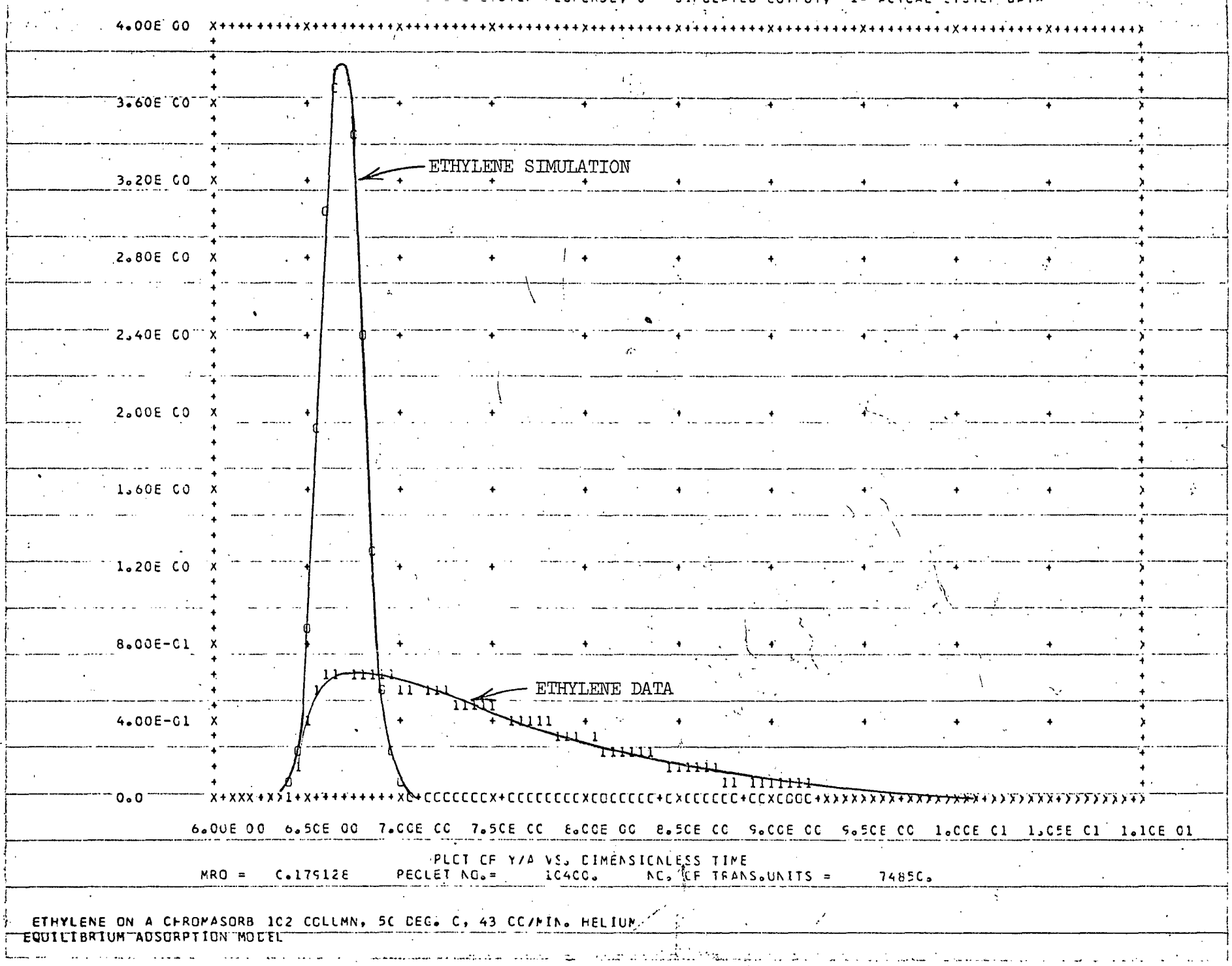

Figure 3 Comparison of Predicted and Actual Chromatograms for Ethylene on Chromosorb 102 at 50°C

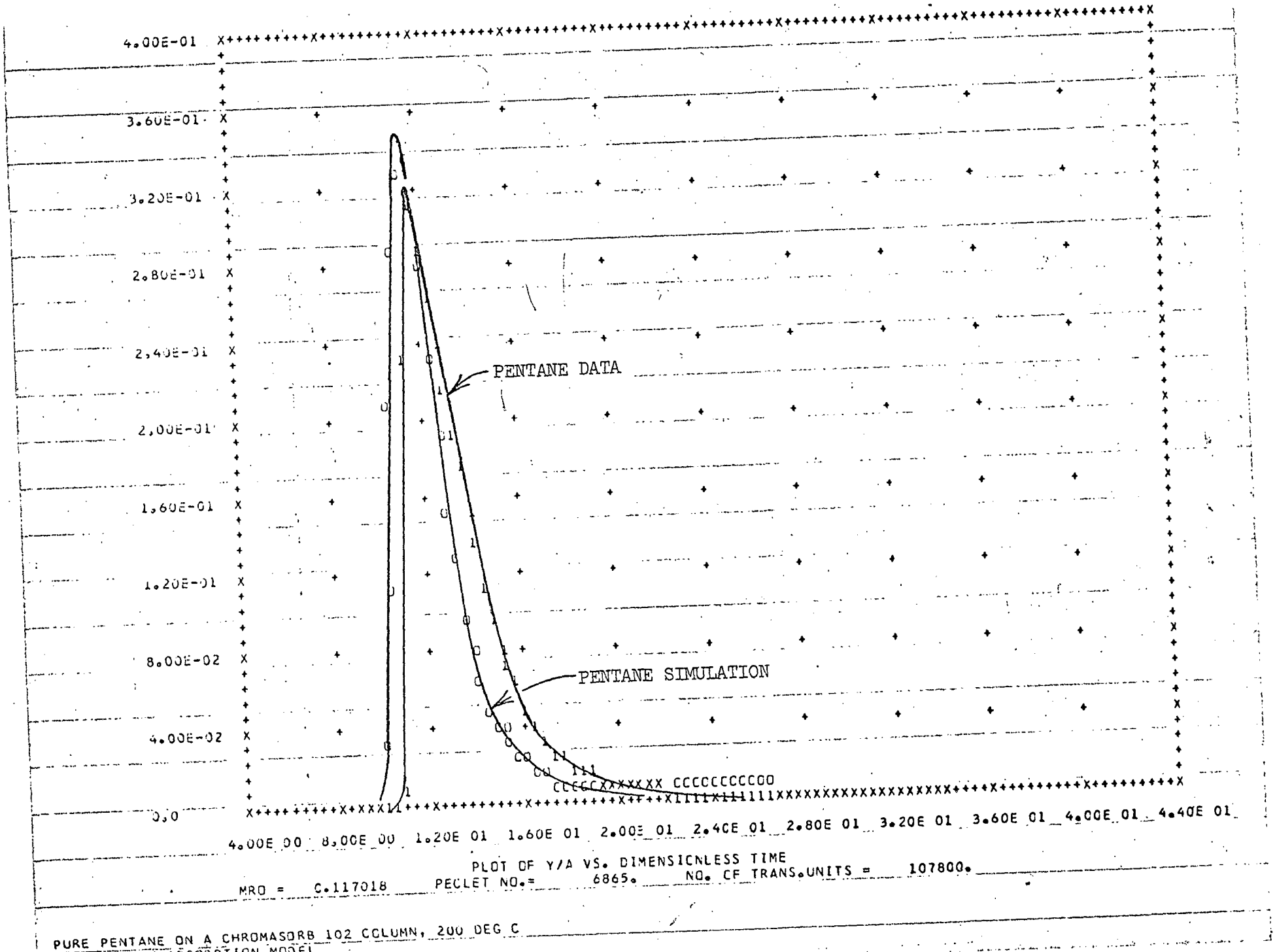

Figure 4 Comparison of Predicted and Actual Chromatograms for Pentane on Chromosorb 102 at 200°C

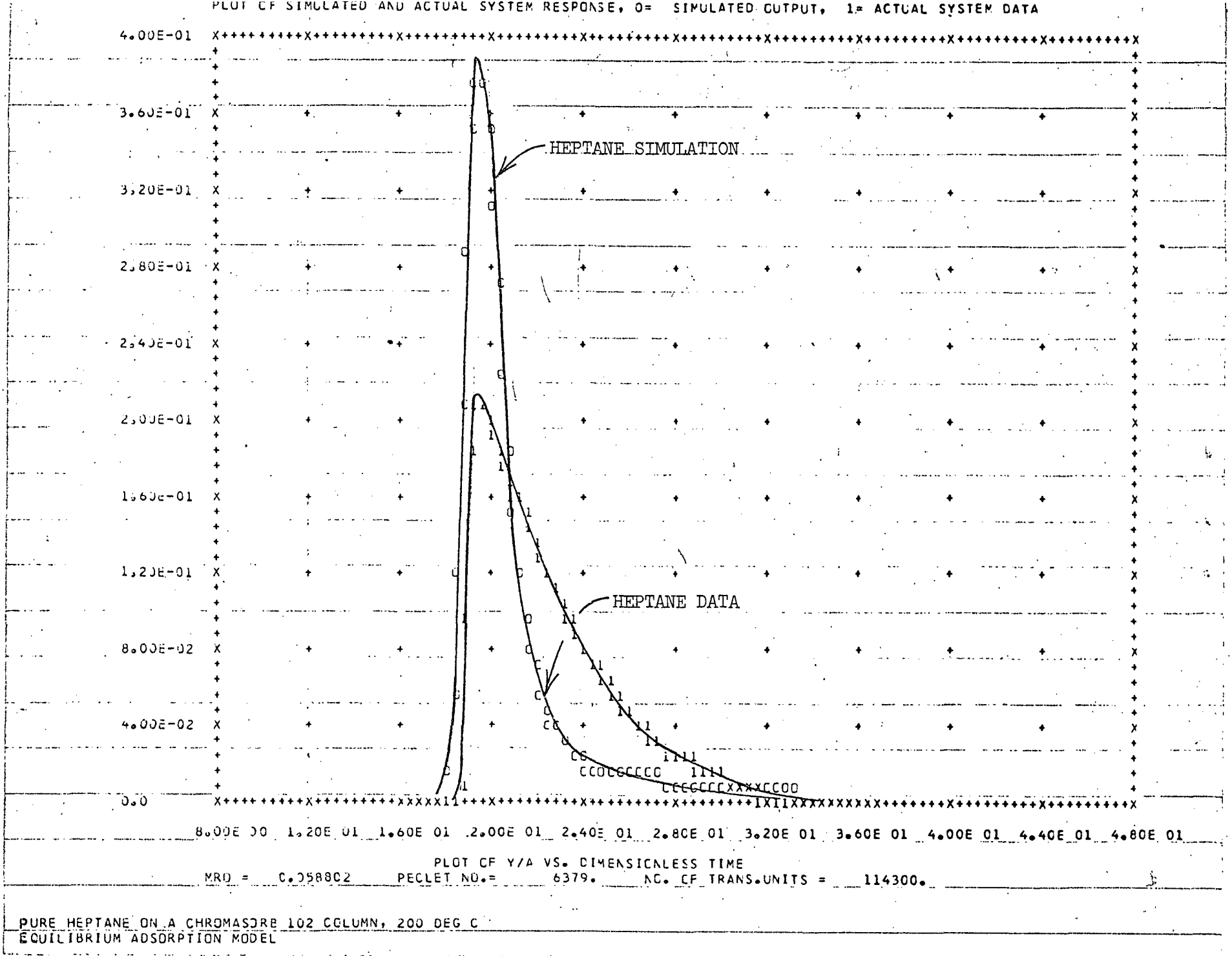

Figure 5 Comparison of Predicted and Actual Chromatograms for Heptane on Chromosorb 102 at 200°C

TABLE VII

COMPARISON OF EQUILIBRIUM AND NON-EQUILIBRIUM ADSORPTION MODELS WITH CHROMATOGRAPHIC DATA

System	Column	Equilibrium Model Avg. Squared Dev.	Non-Equilibrium Model Avg. Squared Dev.
Nitrogen, 20°C	Molecular Sieve	0.00743	0.00741
Oxygen, 20°C	"	0.00486	0.00570
Pentane, 150°C	Chromosorb 102	0.000575	0.000580
Pentane, 200°C	"	0.000192	0.000195
Heptane, 150°C	"	0.000481	0.000464
Heptane, 200°C	"	0.000228	0.000202
Acetone, 125°C	"	0.000877	0.000863
Acetone, 100°C	"	0.0000386	0.0000387
Acetone, 125°C	"	0.0000266	0.0000270
Acetone, 150°C	"	0.0000104	0.0000108
Acetone, 175°C	"	0.0000051	0.0000046
Acetone, 200°C	"	0.0000457	0.0000406
Ethylene, 20°C	"	0.0130	0.0122
Ethylene, 28°C	"	0.0141	0.0132
Ethylene, 50°C	"	0.0296	0.0283
Ethylene, 75°C	"	0.0560	0.0539
Ethylene, 100°C	"	0.0747	0.0730
Ethylene, 125°C	"	0.0797	0.0781
Ethylene, 150°C	"	0.0867	0.0853
Ethylene, 175°C	"	0.0828	0.0769

made previously; in particular the following may be said:

1. Both models perform very similarly with respect to prediction of output chromatograms.
2. The predictions for the acetone systems are superior to predictions for other systems.
3. Predictions for the ethylene systems are the worst of all.
4. The improvement in prediction by including a finite N_{tOG} in system modeling is at best minor, at least for the conditions studied. Equilibrium adsorption implies an infinite value for N_{tOG}, whereas in the experiments summarized in Table V, the value ranged from 62,000 to 148,000. It appears for these values of N_{tOG} that adsorption equilibrium is approached. Under other circumstances, e.g., with a much shorter column, the terms involving N_{tOG} will have much more influence on the prediction.
5. Within each system group, especially acetone and ethylene the quality of prediction depends strongly upon temperature. For acetone, heptane and pentane, the model representation improves, whereas for ethylene, the trend is opposite. This implies different mechanisms controlling the adsorption-desorption-transport process are involved and that further model improvement is required.

The present models represent fairly well the chromatograms of acetone, pentane, and heptane on Chromosorb 102. In the light gas systems -- ethylene, nitrogen, and oxygen -- agreement between the theoretical prediction and experimental data are not as satisfactory. Experimental chromatograms show more dispersion than the simulations,

and hence suggest other transport processes or capacitances have not been included in the model. It is noted that the adsorbent used, Chromosorb 102 in most cases and Molecular Sieve 5A in two experiments are porous. The lighter materials, such as ethylene, nitrogen, and oxygen, may adsorb internally within the adsorbent particles, whereas the larger acetone, pentane and heptane may be confined to the external adsorbent surface. Thus the process of intraparticle diffusion, which was neglected in the model derivation, may be appreciable and hence responsible for the observed discrepancies.

This additional mechanism is further suggested from an examination of the temperature behavior of the thermodynamic parameter mR_0. Table VIII summarizes the temperature effect on this parameter for both the acetone and ethylene systems. Although these values of the parameter were obtained from evaluating the two models under consideration, earlier work (2,3) showed that mR_0 is the primary factor affecting the time when the maximum composition in the chromatogram appears. As a first-order approximation, the value of mR_0 is probably independent of the transport processes involved as long as the linear isotherm, Equation 3, is used, and hence the data of Table VIII are reasonable representations of the actual adsorption process. Approximate temperature correlations for these data appear in Figures 6 and 7. Over the temperature range considered, the activation energy E for mR_0, as defined in the following equation

$$mR_0 \sim \exp(-E/RT)$$

is of the order of 6 kcal/gm-mole for the acetone system, an indication that the controlling mechanism is probably a physical adsorption process

TABLE VIII

THERMODYNAMIC PARAMETER DATA FOR
ACETONE AND ETHYLENE ON CHROMOSORB 102

Component	Parameter mR_0	Temperature T, deg K	1000/T
Acetone	0.0286	373	2.68
	0.0576	398	2.51
	0.0527	398	2.51
	0.0968	423	2.36
	0.122	448	2.23
	0.173	473	2.11
Ethylene	0.112	301	3.32
	0.194	323	3.10
	0.320	348	2.88
	0.423	373	2.68
	0.479	398	2.51
	0.601	423	2.36
	0.587	448	2.23

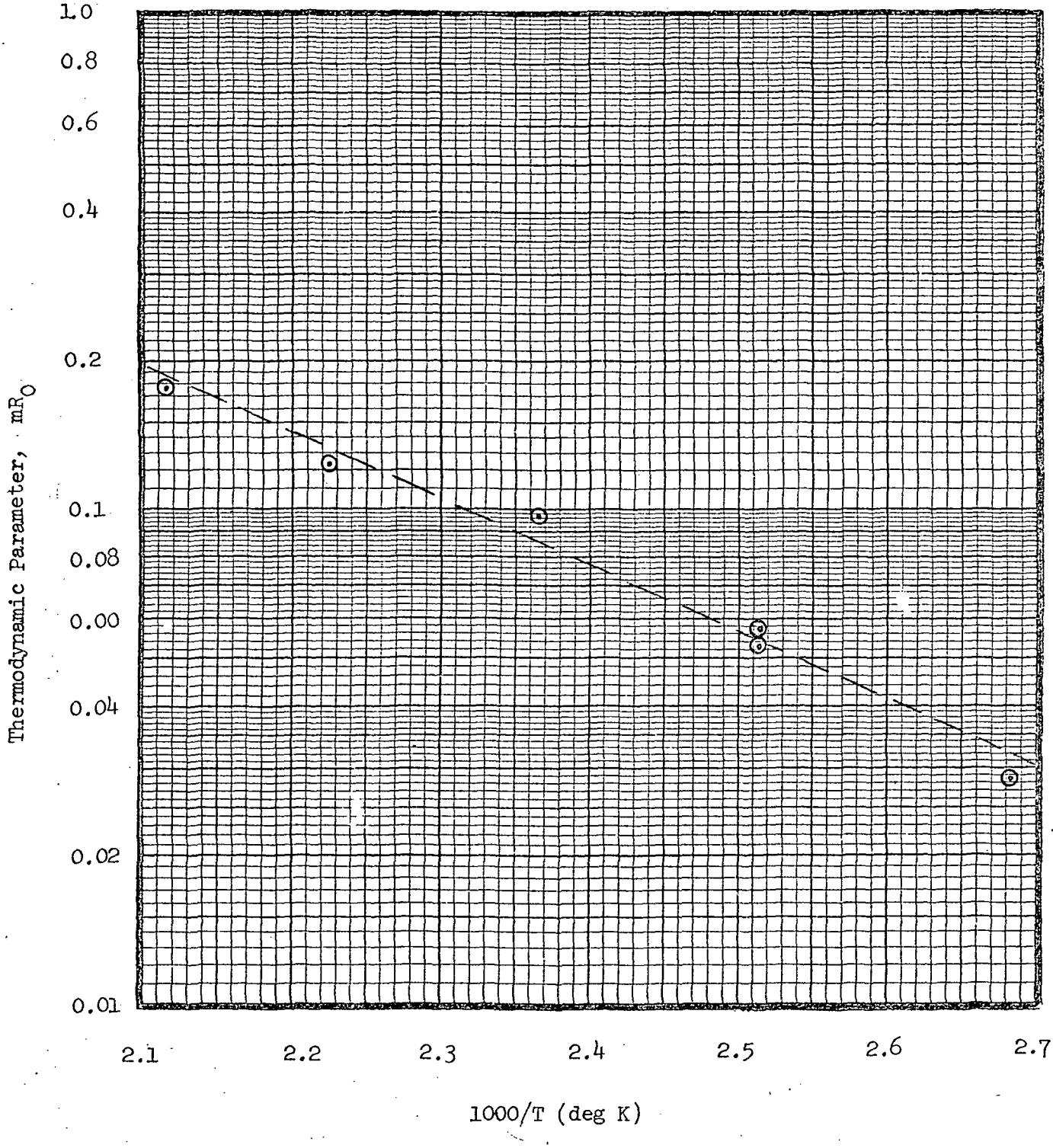

Figure 6 Effect of Temperature on Parameter mR_O for Acetone

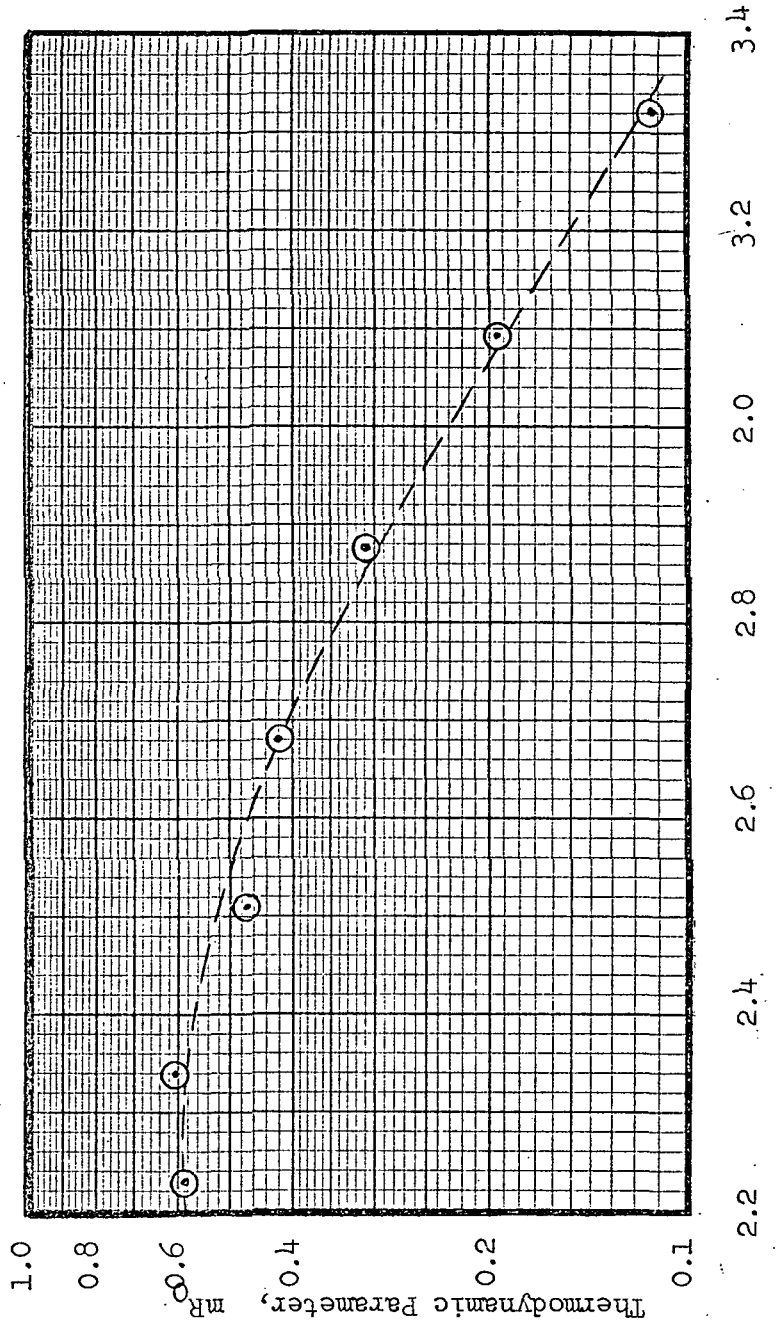

Figure 7 Effect of Temperature on Parameter mR_O for Ethylene

as proposed by the model. For the ethylene system, the corresponding activation energy varies from about 1.5 kcal/mole at 175°C to 4 kcal/mole at 28°C. Intraparticle diffusion (a low activation energy process) superimposed upon physical adsorption (a high activation energy process) would exhibit such temperature behavior, with the adsorption process controlling at the lower temperatures. The effect of temperature upon the quality of prediction for the ethylene data given in Table VII further substantiates such a proposal.

In summary, it appears that the mechanism of intraparticle diffusion must be considered if the mathematical model is to be improved. Consideration of this diffusion further complicates the mathematical models, and a workable, analytical solution may not be obtained. If this is the case, direct numerical techniques will be employed. The resulting mathematical model will subsequently be evaluated with the experimental data to establish the importance of this mechanism. Further, experiments with an adsorbent which is not appreciably porous would appear in order. It is believed that the Carbowax 1500 column described in Table IV is considerably less porous and is better represented by the system equations of the currently studied model. Further experimental work with this adsorbent is planned.

F. Experimental Conditions - Binary System Studies

Superposition was studied with the binary system n-pentane/n-heptane which is representative of a heavy organic system. A Chromosorb 102 column, described in Table IV, was used and the liquid mixture was vaporized during the injection and prior to entering the column. Table IX summarizes the experimental conditions. Data were obtained at 150 and 200°C and the composition of the sample was varied from an excess of one component to an excess of the other.

TABLE IX

EXPERIMENTAL CONDITIONS: BINARY SYSTEM STUDIES

Pentane-Heptane System on a Chromosorb 102 Column
Sample Size: Two microliters

Pentane Composition weight percent	Helium Flowrate cu cm/min	Temperature deg C
1	32.2	150
25	32.2	150
50	32.2	150
75	32.2	150
99	32.2	150
1	20.0	200
25	20.0	200
50	20.0	200
75	20.0	200
99	20.0	200

G. Binary System Results and Superposition

Figures 8 through 12 show typical comparisons between the experimental chromatograms at 200°C and model simulations. The predicted chromatograms are derived from the Equilibrium Adsorption Model using pure component data (mR_0) and the convolution procedure of Benoit (4) together with superposition. Similar figures and selected tabular data for all experiments appear elsewhere (5). Pure component data at 200°C appear in Figures 4 and 5.

Figure 8 shows the results for a mixture having 50% by weight pentane. It is apparent that the experimental data lag the predicted data in time for both components. Figure 9 shows the results for a mixture containing 1% by weight pentane. Because of the particular composition scale used, the pentane peaks do not appear. Figure 10 shows these predicted and observed pentane peaks on an expanded scale. Again, a time lag exists between the simulation and experimental chromatogram. Figures 11 and 12 show similar results for a mixture containing 1% by weight heptane.

In this binary system, actual data lag the predicted curves over the entire composition range and for both temperatures considered, 150 and 200°C. Tables X and XI summarize these results. It is noted that these deviations are slightly more pronounced at the lower temperature. It is also evident that as the component composition in the sample becomes less, the time lag becomes greater. This occurs for both pentane and heptane.

Earlier work (2,3) showed the parameter mR_0 is the primary factor affecting the time when the maximum composition appears. The fact that the peak occurs at a different time for each sample composition

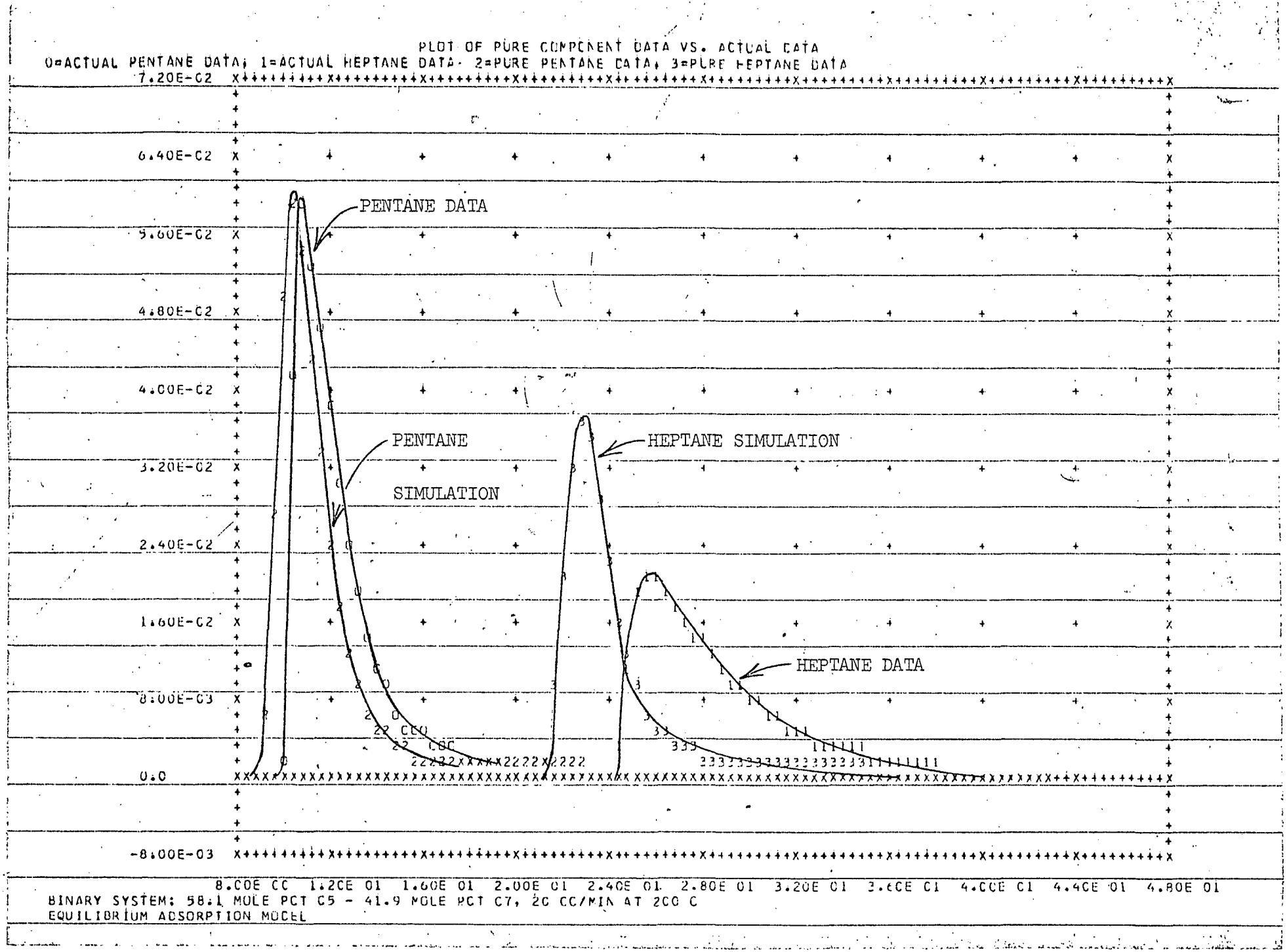

Figure 8 Pentane-Heptane System on Chromosorb 102 at 200°C

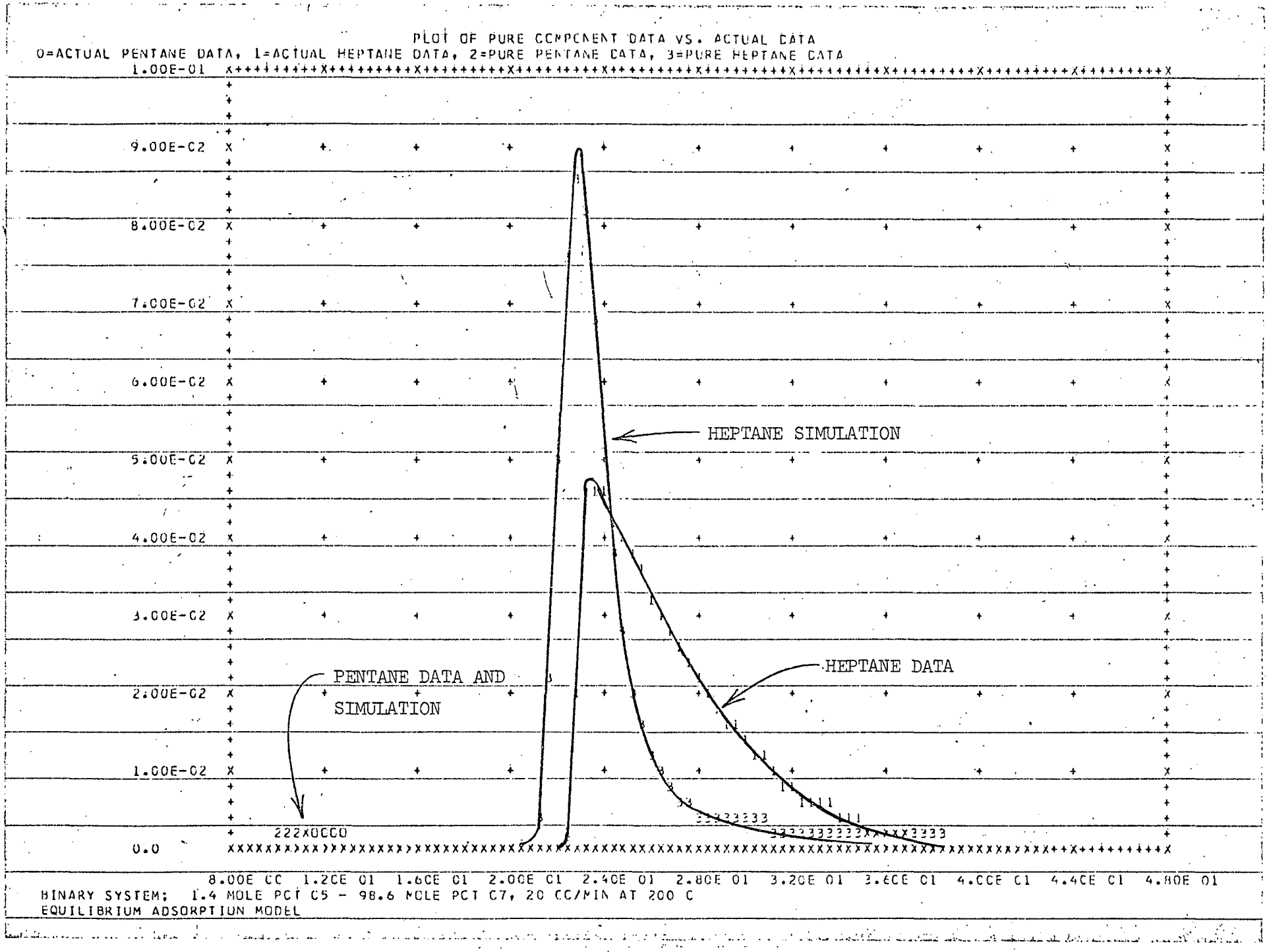

Figure 9 Pentane (dilute)-Heptane System on Chromosorb 102 at 200°C: System Chromatograms

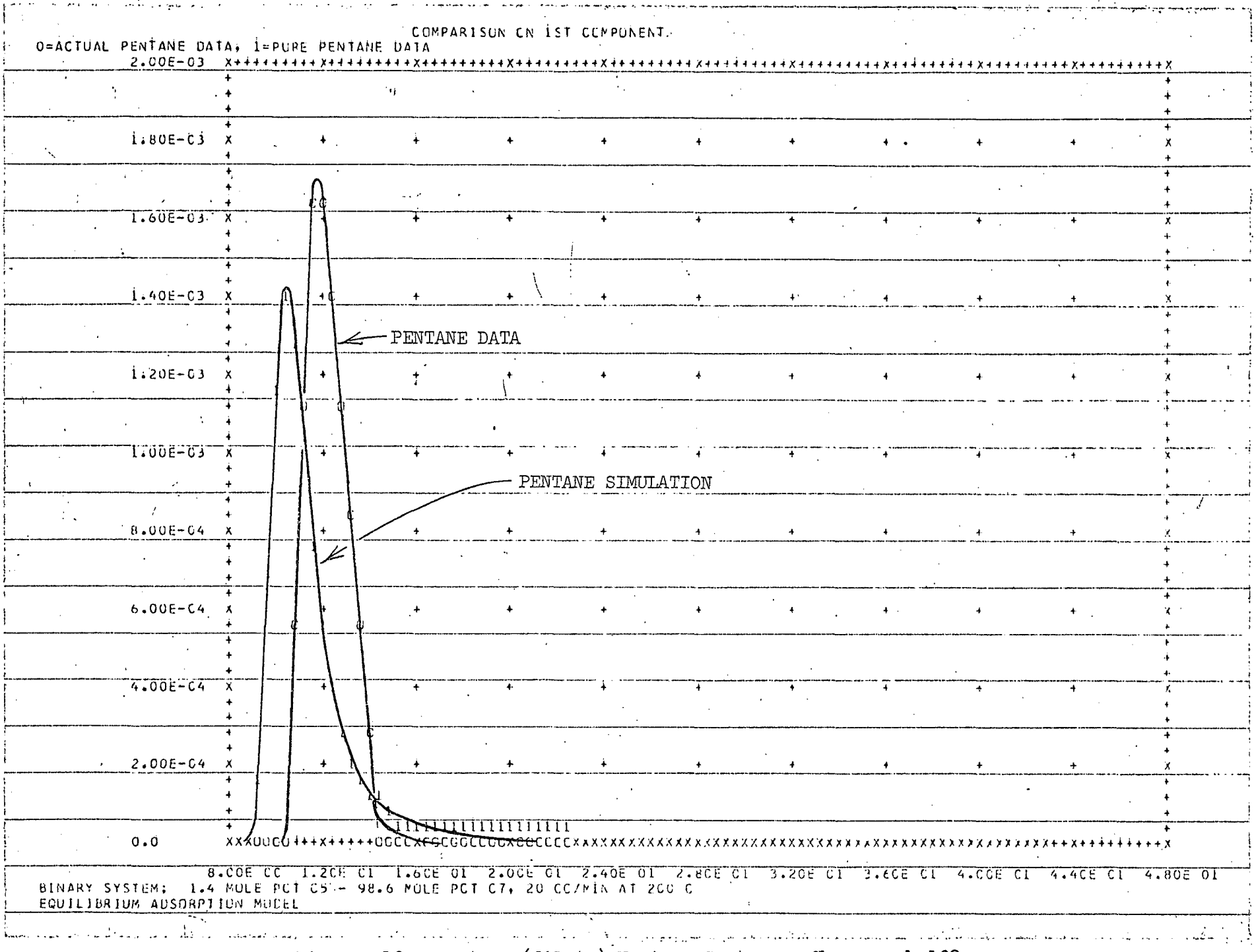

Figure 10 Pentane (dilute)-Heptane System on Chromosorb 102 at 200°C: Pentane Chromatograms

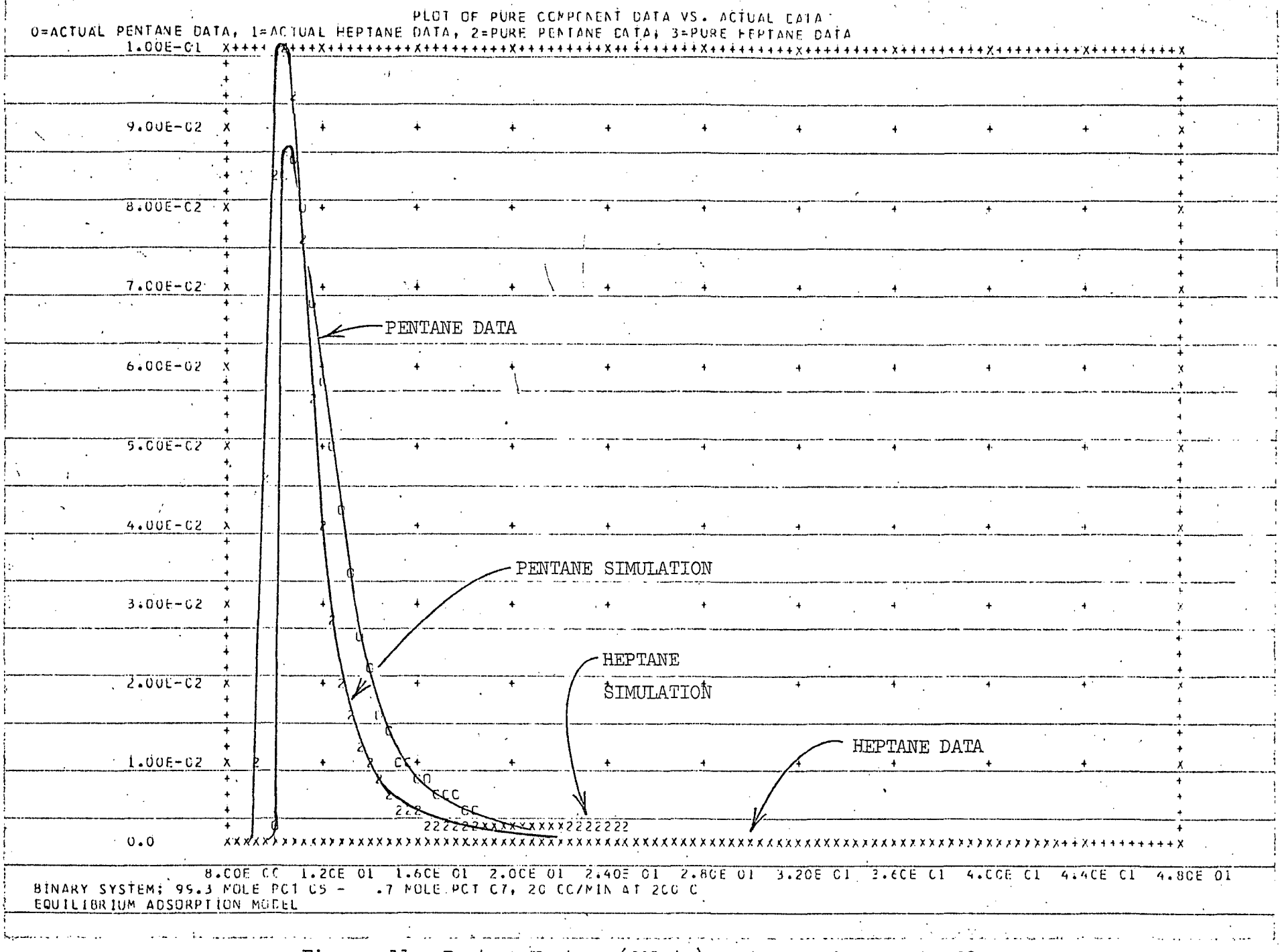

Figure 11 Pentane-Heptane (dilute) System on Chromosorb 102 at 200°C: System Chromatograms

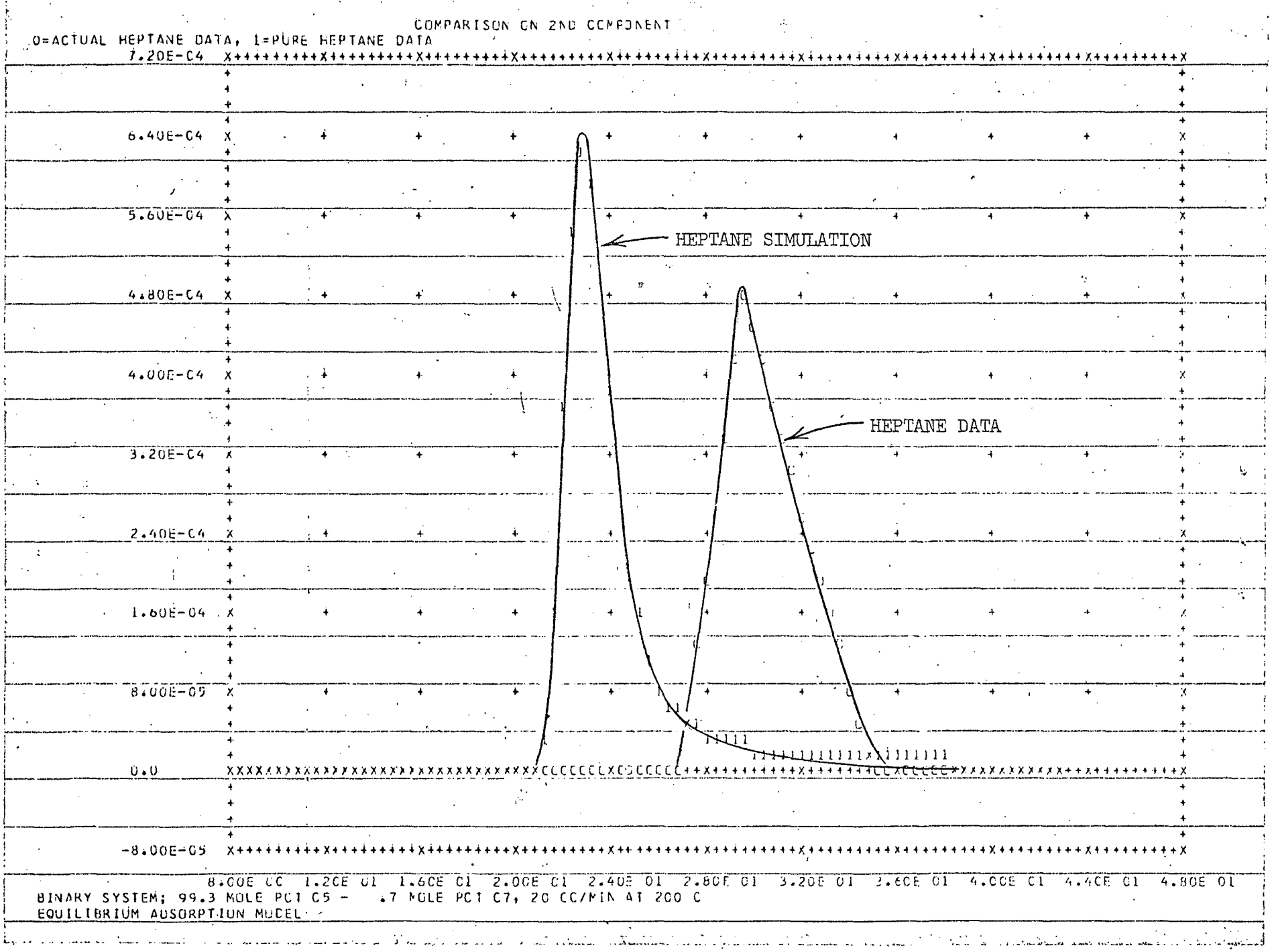

Figure 12 Pentane-Heptane (dilute) System on Chromosorb 102 at 200°C: Heptane Chromatograms

TABLE X

EVALUATION OF SUPERPOSITION

Pentane-Heptane System on Chromosorb 102 Column at 150°C

Pentane Composition weight percent	Pentane Peak seconds	Heptane Peak seconds
0	—	122.5
1	47.5	121.5
25	44.0	126.5
50	42.4	138.5
75	39.5	144.0
99	40.0	174.0
100	40.0	—

TABLE XI

EVALUATION OF SUPERPOSITION

Pentane - Heptane System on Chromosorb 102 Column at 200°C

Pentane Composition weight percent	Pentane Peak seconds	Heptane Peak seconds
0	—	85.0
1	43.0	86.5
25	41.0	89.0
50	39.5	94.5
75	39.0	102.0
99	38.5	110.0
100	38.5	—

suggests that mR_0 is a function of composition which decreases as the composition of the component decreases (or as the composition of the other component increases). This is not surprising considering the physical processes involved during the adsorption step. Adsorbent surface coverage is an important factor in processes involving the adsorption phenomena such as catalysis, and must be considered. In particular, it is probable that the adsorption isotherm, Equation 3, which assumes no coupling between the components, should perhaps be modified to account for surface coverage or the amount of each component adsorbed.

In summary, it appears that superposition of the basic equations is an idealization, at least for the specific system studied, but it offers a first-order approximation to system behavior. In the immediate future, additional data for the pentane-heptane system will be obtained on the Chromosorb 102 adsorbent at other temperatures in the range of 50 to 200°C. In addition, the behavior of this system with the Carbowax 1500 adsorbent described in Table IV will be studied. As noted before, this column is fundamentally different from the Chromosorb 102 adsorbent and is believed better represented by the system equations currently being studied. These studies will provide data to investigate compositional effects on the term mR_0 and will guide further theoretical work.

VI. CONCLUSIONS AND FUTURE WORK

The following conclusions are derived from the preceding investigation. In addition to offering conclusions, some directions are indicated for future endeavors in the area of chromatographic systems analysis.

1. For the components and conditions analyzed, the Non-Equilibrium Adsorption Model yields at best, minor improvement over the Equilibrium Adsorption Model in output chromatogram prediction.

2. Because of the high values of N_{tOG} encountered, further study is needed to determine effects of lower N_{tOG} on the quality of prediction from these models. Parametric studies are necessary to determine this.

3. The failure of both models to predict the total amount of chromatogram dispersion under certain conditions suggests that a heretofore neglected mechanism, temperature dependent in nature, is present in the overall adsorption-desorption phenomena characteristic of the chromatograph operation. A most likely candidate for subsequent modeling work is the mechanism of intraparticle diffusion. Consideration of this mechanism involves another set of partial differential equations that describe component behavior within the particles of the packing. This additional set of partial differential equations is coupled to the interparticle partial differential equations used previously for model derivations. Chromatographic model improvement will proceed in this direction. Experimental investigations are slated to proceed using a non-porous packing in the chromatograph. This should negate intraparticle diffusion and allow better analysis of the interparticle models and a closer prediction of the data.

4. Superposition of pure component chromatogram predictions yields a good, first-order approximation of binary output data. However, it appears the thermodynamic parameter mR_0 is composition-dependent, decreasing as the composition of its component decreases. Additional data on multicomponent systems and further studies are indicated.

VII. ACKNOWLEDGEMENT

The authors express their sincere thanks to Dr. Peter K. Lashmet, whose comments, advice, and assistance contributed substantially to the completion of this project. Further acknowledgement is made to Dr. G. Paine of JPL, contract monitor, and Dr. S. Yerazunis, project director for Rensselaer, and for their patience and helpful comments. In addition Mr. P.S. Keba acknowledges financial aid from Rensselaer in the form of a graduate teaching assistantship. Mr. P.T. Woodrow acknowledges financial support from Rensselaer and the U.S. Department of Health, Education and Welfare by an NDEA Title IV Fellowship.

VIII. NOMENCLATURE

English Letters

$A\delta$ - unit impulse, Dirac delta function.

a - ratio of interfacial area to packed volume.

d - diameter of packing.

D - effective diffusion or dispersion coefficient.

D_m - molecular diffusivity of sample in carrier gas.

E - activation energy, cal/gm-mole.

F - argument of exponential in integral, Equation 18.

I_0 - modified Bessel function of the first kind, order zero.

I_1 - modified Bessel Function of the first kind, order one.

L - length of chromatograph column.

mR_0 - thermodynamic parameter.

N_{tOG} - number of transfer units, dimensionless.

p - probability parameter in Peclet number correlation.

Pe - Peclet number, dimensionless

p_i - pressure at column inlet.

p_o - pressure at column outlet

R - gas constant, 1.987... cal/(gm-mole, ^oK)

Re - Reynolds number based on particle diameter and superficial velocity, dimensionless

R_0 - ratio of moles of gas to moles of adsorbed in bed.

Sc - Schmidt number, dimensionless.

Sh - Sherwood number, dimensionless.

T - temperature, degrees K.

t - time; argument in Bessel function approximation.

v - corrected average superificial velocity

$\bar{v}$ - interstitial velocity = v/ϵ

v_{avg} - superificial velocity based on average column pressure

x - concentration in adsorbent phase, dimensionless; variable of integration.

y - concentration in vapor phase, dimensionless.

y^* - concentration in vapor phase at equilibrium, dimensionless.

z - dimensionless axial position in column.

Greek Letters

α_1 - first eigenvalue of $J_0 = 2.40482...$

β - $1 + 1/mR_0$

Γ - $4(1-\epsilon)\ \alpha_1^2/\epsilon$

ϵ - bed porosity

ρ - density of carrier gas.

μ - viscosity of carrier gas.

π - constant = 3.14159...

τ - tortuosity factor.

θ - dimensionless time = $\bar{v}t/L$.

IX. REFERENCES

1. Sliva, T.F., "Chromatographic Systems Analysis: First Order Model Evaluation," RPI Technical Report MP-1, Rensselaer Polytechnic Institute, Troy, New York, Sept. 1968.

2. Voytus, W.A., "Chromatographic Systems Analysis: Moment Analysis of the Equilibrium Adsorption Model," RPI Technical Report MP-9, Rensselaer Polytechnic Institute, Troy, New York, Aug. 1969.

3. Taylor, P.N., "Chromatographic Systems Analysis: Second Order Model Development," M. Eng. Report, Rensselaer Polytechnic Institute, Troy, New York, June 1970.

4. Benoit, G.L., "Reduction of Chromatographic Data and Evaluation of a GC Model," RPI Technical Report MP-22, Rensselaer Polytechnic Institute, Troy, New York, June 1971.

5. Keba, P.S., and Woodrow, P.T., "A Comparison of Two Gas Chromatograph Models and Analysis of Binary Data," M. Eng. Report, Rensselaer Polytechnic Institute, Troy, New York, June, 1972.

6. Lapidus, L., and Amundson, N.R., "Mathematics of Adsorption in Beds. VI. The Effect of Longitudinal Diffusion in Ion Exchange and Chromatographic Columns," J. Phys. Chem., 56, 984-988 (1952).

7. Abramowitz, M., and Segun, I.A., "Handbook of Mathematical Functions," Dover, New York, 1965, p. 378.

8. Conte, S.D., "Elementary Numerical Analysis," McGraw-Hill, New York, 1965, pp. 131, 52.

9. Lashmet, P.K., "Notes on Average Velocity in Chromatographic Column," private communication, May 1972.

10. Wilke, C.R., and Lee, C.Y., "Estimation of Diffusion Coefficients for Gases and Vapors," Ind. Eng. Chem., 47, 1253-1257 (1955).

11. Hirschfelder, J.O., Bird, R.B., and Spotz, E.L., "The Transport Properties for Non-Polar Gases," J. Chem. Phys., 16, 968-981. (1948).

12. Bird, R.B., Hirschfelder, J.O., and Curtiss, C.F., "Theoretical Calculations of the Equation of State and Transport Properties of Gases and Liquids," Trans. ASME, 76, 1011-1038 (1954).

13. Gunn, D.J., "Theory of Axial and Radial Dispersion in Packed Beds," Trans. Inst. Chem. Eng., 47, T351-T359 (1969).

14. Wakao, N., Oshima, T., and Yagi, S., "Mass Transfer From Packed Beds of Particles to a Fluid," Kagaku Kogaku, 22, 780-785 (1958).

15. Scheid, F., "Numerical Analysis," McGraw-Hill, New York, p. 318, (1968).